Temperature driven nano-domain evolution in lead-free $Ba(Zr_{0.2}Ti_{0.8})O_3$-$50(Ba_{0.7}Ca_{0.3})TiO_3$ piezoceramics

Shengbo Lu,[1,a)] Zhengkui Xu,[1] Shi Su,[2] and Ruzhong Zuo[2]
[1]*Department of Physics and Materials Science, City University of Hong Kong, Kowloon, 83 Tat Chee Avenue, Kowloon, Hong Kong, China*
[2]*Institute of Electro Ceramics and Devices, School of Materials Science and Engineering, Hefei Unviersity of Technology, Tunxi Road 193, Hefei 230009, China*

(Received 11 May 2014; accepted 20 July 2014; published online 25 July 2014)

Hierarchical micro- and nanoscale domain structures in Pb-free $Ba(Zr_{0.2}Ti_{0.8})O_3$-$50(Ba_{0.7}Ca_{0.3})TiO_3$ piezoceramics were investigated by transmission electron microscopy. *In situ* heating and cooling studies of domain structure evolution reveal an irreversible domain transformation from a wedge-shaped rhombohedral nanodomain structure to a lamellar tetragonal domain structure, which could be associated with strong piezoelectricity in $Ba(Zr_{0.2}Ti_{0.8})O_3$-$50(Ba_{0.7}Ca_{0.3})TiO_3$ piezoceramics.
 [http://dx.doi.org/10.1063/1.4891756]

Lead-free piezoceramics have attracted much attention due to their non-toxicity in nature and comparable piezoelectric properties with the popular $Pb(Zr,Ti)O_3$ (PZT) ceramics.[1–4] A series of material systems, such as $BaTiO_3$ (BT),[5,6] $(Bi,Na)TiO_3$ (BNT),[7,8] and $(K,Na)NbO_3$ (KNN)[9,10] based ceramics, have been extensively investigated to substitute for PZT. One of the most promising lead-free candidates is the pseudobinary ferroelectric system $Ba(Zr_{0.2}Ti_{0.8})O_3$-$x(Ba_{0.7}Ca_{0.3})TiO_3$ or BZT-xBCT (x is the molar percent of BCT), which was first reported by Liu and Ren in 2009.[11] A very high longitudinal piezoelectric coefficient d_{33} of 620 pC/N at room temperature, which is comparable with high-end PZT, is achieved at a composition of BZT-50BCT locating in proximity to a ferroelectric-ferroelectric morphotropic phase boundary (MPB) of this system. Nevertheless, one drawback of the BZT–xBCT system is its low Curie temperature (T_C). Even the optimal composition, BZT–50BCT, has a T_C of only 93 °C,[11] which may restrict its applications. The strong piezoelectric response has been interpreted in terms of isotropic flattening of a free energy profile associated with the paraelectric cubic-ferroelectric rhombohedral-ferroelectric tetragonal (C-R-T) triple point which is also a tri-critical point. Therefore, great efforts have been devoted to studying the temperature induced structure change of the BZT-xBCT system to elucidate the origin of this large piezoelectricity by *in-situ* x-ray diffraction (XRD)[12,13] and Raman scattering.[14,15] Transmission electron microscopy (TEM), on the other hand, has a very high spatial resolution compared to XRD and Raman scattering, and thus can provide accurate structure information at nanometer scale, particularly with the convergent beam electron diffraction (CBED) technique. Recently, Gao *et al.*[16,17] reported the coexisting nano-scale tetragonal and rhombohedral domains in BZT-50BCT, and the domain structure contribution to the piezoelectric property has also been discussed. Their study indicates that the phase instabilities only cannot explain the origin of strong piezoelectricity and other factors such as the domain wall contribution should be considered. It has been well established that up to 40% of the total direct longitudinal piezoelectric coefficient d_{33} of coarse grained BT and PZT with the MPB composition ceramics was due to the motion of domain walls.[18–20] As a result, it is important to understand how domain walls move under thermal cycle and electric field. Although temperature dependence of domain configuration was reported by Gao *et al.*,[16] their focus was not on the displacement of domain walls and its effect on the macro-properties. The temperature driven domain evolution and its effect on the macro-property of the material remain unclear. In this Letter, a hierarchical micro- and nanoscale domain structures in BZT-50BCT is further studied by TEM and thermally induced evolution of this hierarchical domain is examined by *in situ* heating and cooling, which reveals the irreversible displacement of domain walls during heating and cooling. In addition, a remanent piezoelectric property at temperatures above T_C is observed, which is ascribed to the sustained submicron domains in the temperature range.

BZT-50BCT ceramics were fabricated by a conventional solid-state reaction method with starting chemicals of $BaCO_3$ (≥99%), $CaCO_3$ (≥99%), ZrO_2 (≥99%), and TiO_2 (≥99%). Calcination was done at 1350 °C for 3 h followed by sintering at 1450 °C for 3 h. The specimens for TEM observation were prepared from bulk materials by mechanical thinning to ~10 μm and then ion milling to perforation using a Gatan Dual Ion mill unit (Model 600). Specimens were coated with carbon before TEM examination. The domain morphology was examined on TEM (Philips CM-20, Hillsboro, OR) operated at 200 kV. The *in situ* heating/cooling observation was performed from room temperature to 120 °C on a double-tilt heating specimen holder (Gatan Model 652) with the temperature controlled precisely by a SmartSet Hot Stage controller (Gatan Model 901). The accuracy of the temperature measurement is about 0.1 °C. Heating and cooling rates less than 3 °C/min were used. Images and CBED patterns were recorded 10 min after the temperature was stabilized. The selected area electron diffraction (SAED) and CBED patterns are indexed on the basis of the pseudo-cubic unit cell. All specimens were annealed at a temperature of 80 °C for 24 h to release the stress induced during sample preparation. Polarization versus electric field (P-E) hysteresis loops were measured at different

a)Electronic mail: shengbo.lu@yahoo.com

temperatures using a ferroelectric measuring system (Precision LC, Radiant Technologies, Inc. Albuquerque, NM, USA). The longitudinal piezoelectric coefficient d_{33} was measured by a Belincourt-meter (YE2730A, Sinocera, Yangzhou, China). The planar electromechanical coupling factor k_p was determined by a resonance-antiresonance method with an impedance analyzer (Impedance Analyzer, PV70A, Beijing, China).

Figure 1 shows the bright field images of typical domains of BZT-50BCT taken a few degrees off the [001] zone axis in order to view the nanodomains clearly. Many nanodomains with an average width of 10 nm are assembled into wedge-shaped submicron domains, as evident in Fig. 1(a), which have been noted in both Pb-free and Pb-based systems as "hierarchical domain morphology."[16,21–27] In addition, there exist parallel lamellar domains with an average width of 50 nm marked by the dash lines in Fig. 1(a), which lie perpendicular to the nanodomains within the wedge shaped domains. The SAED pattern obtained from an area covered several submicron domains is shown in the inset of Fig. 1(a), indicating that the projection traces of nanodomain walls inside the wedge shaped domains and the parallel lamellar domains are approximately along [110] and [1–10] directions, respectively. The domain walls of the wedge-shaped subdomains are approximately along [100] and [010] directions, as indicated by the solid lines in Fig. 1(a). Fig. 1(b) shows the wedge-shaped domains with an interwoven structure of two sets of domains. It is noted that these wedge-shaped also consist of many curved lamellar domains inside. The domain walls in this type of domain can be attributed to neither {100} nor {110}. This is similar to the domain structure observed in $Pb(Mg_{1/3}Nb_{2/3})O_3$-$PbTiO_3$ (PMN-PT) crystals as reported recently.[28] More interestingly, curved domain walls are observed, as marked by white arrows in Figs. 1(a) and 1(b). It has been studied by neutron diffraction recently that the Ca substitution on Ba sites will enhance octahedral tilting of ZrO_6 in BZT-50BCT, resulting in a non-uniform lattice distortion.[29] The variation in stress at these localized area can affect the positions of the domain walls as domain walls are created to minimize the elastic and electric stresses associated with the transition from a paraelectric to a ferroelectric phase. Therefore, the curved domain walls are developed in BZT-50BCT similar to the case observed in Pb-based system.

According to literature, wedge-shaped domains are typical domain structures in rhombohedral piezoceramics, such as PZT and BT.[30–32] And the BZT-50BCT ceramics in this study is a MPB composition in which the rhombohedral and tetragonal phase coexist in the system, as proved by previous studies.[11,16,17] Therefore, it is necessary and also of interest to know whether there is a phase difference between the wedge-shaped domain and the lamellar domain since they are major domain structures of the BZT-50BCT ceramic studied in this work. Figures 2(a) and 2(b) show typical [001] zone axis CBED patterns in both zero-order Laue zone (ZOLZ) and whole pattern (WP) recorded from two adjacent lamellar domain and wedge-shaped domain shown in Fig. 1(a), respectively. Both ZOLZ pattern and WP in Fig. 2(a) show a 4 mm diffraction symmetry, indicating a tetragonal phase for the lamellar domain according to the relationship between the diffraction symmetry and point group developed by Buxton *et al.*[33] While for the wedge-shaped domain, only a mirror plane parallel to [110] in both ZOLZ pattern and WP can be seen, corresponding to a rhombohedral phase. This is consistent with previous symmetry studies of BZT-50BCT by CBED method[17] and confirms the coexistence of rhombohedral phase, wedge-shaped domains and tetragonal phase, parallel lamellar domains revealed in this study.

It is known that the important piezoelectric properties of materials critically depend on their domain structure. Therefore, to further understand the domain structure and domain wall contribution to the piezoelectric properties in BZT-50BCT piezoceramics, temperature induced domain structure evolution was examined by *in situ* TEM heating and cooling experiments. Figures 3(a)–3(g) show bright-field TEM images of the same area taken from a [001]-oriented grain during heating/cooling cycle. As shown in Fig. 3(a), the domain walls of the parallel lamellar domains are approximately along {110} planes, while the domain walls of the wedge-shaped domains are along {100} planes, which is confirmed from the SAED pattern of the grain shown in the inset of Fig. 3(e). Upon heating from room temperature to 60 °C, a significant change in domain morphology occurred, as evident in Fig. 3(b). Wedge-shaped domains progressively disappear and nanodomains inside them start to merge and transform into parallel lamellar domains. The width of the lamellar domains ranges from 100 nm to several hundreds of nm. The domain morphology transformation corresponds to a rhombohedral to tetragonal phase transition. It should be noted that the curved domain walls developed at the boundaries where wedge-shaped domains and the parallel lamellar domains intercept, indicating a large strain variation

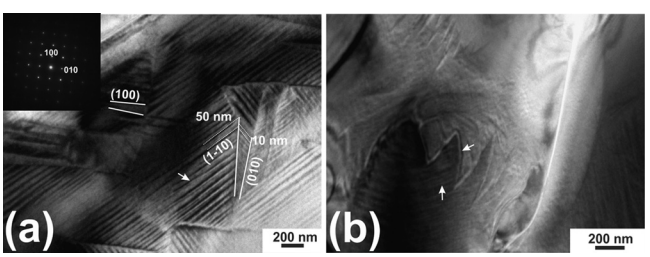

FIG. 1. Bright field images of two typical domain morphologies (a) and (b) with both lamellar domains and wedge-shaped domains in BZT-50BCT, viewed along [001]. Inset of Fig. 1(a) shows the corresponding SAED pattern. White arrows indicate curved domain walls.

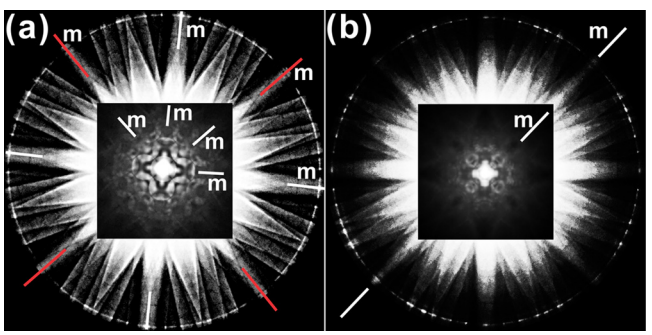

FIG. 2. [001] CBED patterns combined both ZOLZ pattern and WP of BZT-50BCT, taken from (a) lamellar domain, and (b) wedge-shaped domain; (a) and (b) indicate a 4 mm and m diffraction symmetry, respectively.

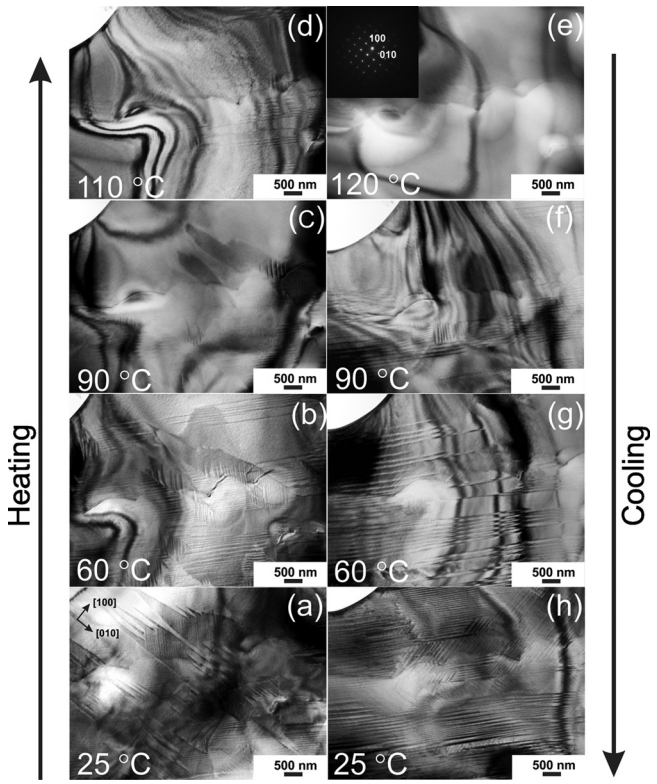

FIG. 3. *In situ* observation of the same area during heating/cooling: (a) hierarchical domains at 25 °C, (b) 60 °C on heating, (c) 90 °C on heating, (d) 110 °C on heating, (e) 120 °C on heating, (f) 90 °C on cooling, (g) 60 °C on cooling, (h) 25 °C on cooling. The inset of (e) shows a [001] SAED pattern of the examined grain.

at two sides of the domain wall. This shows a great similarity to the domain structure of PMN-PT reported recently.[34] It is proposed that the interface between a (100)-type R domain and (110)-type T domain is not strictly a plane but a layer as large lattice distortions could be induced at the R-T interfaces. Accordingly, this distortion can lead to the curvature of the interfaces. When temperature reaches at 90 °C (Fig. 3(c)), the domain contrast is markedly reduced due to the ferroelectric to paraelectric phase transition. However, there still exist some the curved domains and parallel lamellar domains with their traces along [110] and [1–10] directions and the parallel lamellar domains even survived at 110 °C, as shown in Fig. 3(d). The domain contrast completely disappeared at 120 °C, as shown in Fig. 3(e). When temperature is cooled from 120 °C back to 90 °C, lamellar domains with an average size of 100 nm appeared, as evident in Fig. 3(f), which are gradually changed to band submicron domains containing nanodomains at 60 °C (Fig. 3(g)). The bands are along [1–10] direction, while the nanodomains are along [010] direction. After cooling back to room temperature (Fig. 3(h)), the band domains developed into parallel lamellar domains similar to the original ones but with a larger width. However, the wedge-shaped domains do not reappear as the virgin state. This result implies that some domain walls, especially the domains with a rhombohedral phase in BZT-50BCT piezoceramics, are highly mobile and are irreversible when temperature changes. It is speculated that it will be the same case if the ceramic is under an external electric field. Recently, Guo *et al.*[35] reported a unique single-domain state of BZT-50BCT ceramic under an electrical field by *in-situ* TEM. They found that all domain walls disappear when the electric field exceeds a specific level and only small portion of domain walls reappear after removal of the field. Their findings support our speculations. Irreversible displacement of domain walls has been proved to contribute to d_{33} significantly.[18–20] It was found In PZT system that the largest contribution of the irreversible displacement of domain walls to d_{33} is in a rhombohedral composition then followed by a MPB composition and finally a tetragonal composition. Moreover, a Landau-type calculation reveals that in the rhombohedral system a twin boundary on the {110} plane has a surface energy that is only one-third of that of a twin boundary on a {100} plane. And this is why {110} domains are observed to occur more frequently than the higher energy {100} type in rhombohedral PZT syestems.[31] However, the domain walls of wedge-shaped domains with a rhombohedral phase are along {100} plane. The nature of high surface energy makes these {100} type rhombohedral domain walls highly mobile and response easily to temperature and an external electrical field. In addition, due to the mismatch between the coexisting rhombohedral and tetragonal nanodomains, a large non-uniform distortion will be induced at the boundary of the adjacent rhombohedral and tetragonal nanodomains as proved by the curved domain walls found at the interface of rhombohedral and tetragonal nanodomains. During heating and cooling cycles, these non-uniform transformation strains will be redistributed, which will lead to an irreversible displacement of domain walls. It turns out that other than the existence of the miniaturized nanodomains at a MPB composition, the irreversible displacement of domain walls could be another origin of the strong piezoelectricity in BZT-xBCT systems.

Figures 4(a) and 4(b) show the temperature dependence of longitudinal piezoelectric coefficient d_{33}, the planar electromechanical coupling factor k_p, and P-E hysteresis loops. d_{33}, k_p, and remanent polarization P_r all drop as temperature rises and a sudden drop can be seen when temperature reaches 80–90 °C. It is worthwhile to note that there are still noticeable d_{33} and P_r remaining in this temperature range and even a "tail" of d_{33} remains in the temperature range of 90–120 °C, which is close or above the reported T_C, 93 °C. This is consistent with our *in situ* heating observation of domain evolution, in which a large density of nanodomains disappeared at 90 °C but some of the larger submicron domains survived even at 110 °C. They disappeared completely at 120 °C, which is in agreement with macro-property measurement. Unlike the parent ceramic, BT, the submicron domains in BZT-50BCT did not disappear completely as temperature reaches or even exceeds T_C. First, this could result from the Ca substitution on Ba sites. As aforementioned, this substitution could enhance the distortion of ZrO_6 octahedron[29] and could induce the formation of short bond between Ca and O atoms which will further enhance the tetragonal distortion of the BZT-50BCT unit cell, resembling Pb-O bond in $PbTiO_3$.[36] Therefore, the off-centering of Ti/Zr will be more stabilized in BZT-50BCT than in BT. Second, domain wall pinning effect induced by localized dislocations or variations of point defects could be another reason for the sustained submicron domains. The existence of pinning defects is characterized by the bended domain walls around the pinning

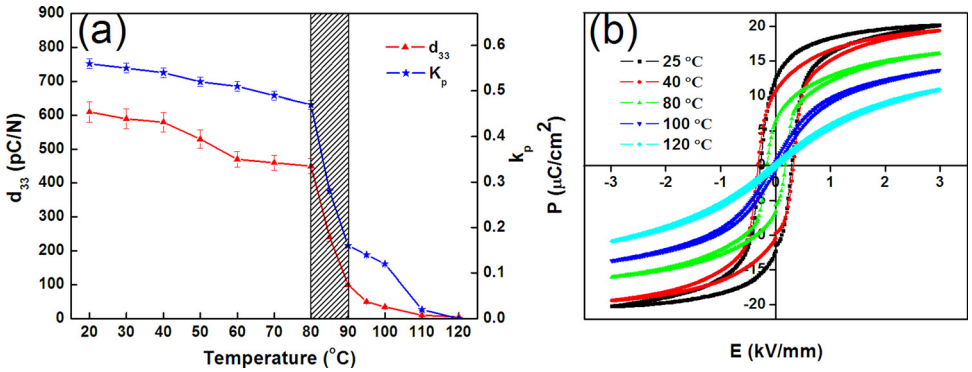

FIG. 4. Temperature dependence of (a) longitudinal piezoelectric coefficient d_{33}, the planar electromechanical coupling factor k_p and (b) P-E hysteresis loops.

defects as evident in Fig. 3(d), which is consistent with the earlier study.[37] They could form defect-dipole complex and generate an internal field which could hinder the recovery of off-centered Ti/Zr atoms to their original position at elevated temperatures. As a result, some local domains sustain at temperatures close or even above T_C, resulting in a noticeable remanent bulk properties at the temperatures above T_C.

In conclusion, our TEM studies reveal the hierarchical micro- and nanoscale domain structures in BZT-50BCT and the coexistence of the lamellar tetragonal domains and wedged-shaped rhombohedral nanodomains. Curved domain walls are generated to accommodate the large non-uniform strain induced by mismatch at the boundary of tetragonal and rhombohedral nanodomains. The redistribution of this non-uniform strain during heating and cooling cycles together with the high mobility of {100} type rhombohedral domain walls lead to an irreversible displacement of the nanodomain walls, which is believed to be associated with the outstanding piezoelectric properties of the BZT-50BCT piezoceramics. Moreover, part of submicron domains sustain in the temperature range that is close or above the T_C, which is responsible for the observed remanent piezoelectric property at temperatures above T_C.

The work was supported by a grant from the Research Grants Council of the Hong Kong Special Administrative Region, China (Project No. 9041211).

[1]P. K. Panda, J. Mater. Sci. **44**, 5049 (2009).
[2]T. R. Shrout and S. J. Zhang, J. Electroceram. **19**, 113 (2007).
[3]S. O. Leontsev and R. E. Eitel, Sci. Technol. Adv. Mater. **11**, 044302 (2010).
[4]D. Maeder, D. Damjanovic, and N. Setter, J. Electroceram. **13**, 385 (2004).
[5]T. Karaki, K. Yan, and M. Adachi, Appl. Phys. Express. **1**, 111402 (2008).
[6]Y. Huan, X. H. Wang, J. Fang, and L. T. Li, J. Am. Ceram. Soc. **96**, 3369 (2013).
[7]T. Takenaka, K. Maruyama, and K. Sakata, Jpn. J. Appl. Phys., Part 1 **30**, 2236 (1991).
[8]T. Takenaka, K. O. Sakata, and K. O. Toda, Ferroelectrics **106**, 375 (1990).
[9]E. Ringgaard and T. Wurlitzer, J. Eur. Ceram. Soc. **25**, 2701 (2005).
[10]Y. Saito, H. Takao, T. Tani, T. Nanoyama, K. Takatori, T. Homma, T. Nagaya, and M. Nakamura, Nature **432**, 84 (2004).
[11]W. F. Liu and X. B. Ren, Phys. Rev. Lett. **103**, 257602 (2009).
[12]Y. Tian, L. L. Wei, X. L. Chao, Z. H. Liu, and Z. P. Yang, J. Am. Ceram. Soc. **96**, 496 (2013).
[13]Y. Tian, X. L. Chao, L. Jin, L. L. Wei, P. F. Liang, and Z. P. Yang, Appl. Phys. Lett. **104**, 112901 (2014).
[14]D. Damjanovic, A. Biancoli, L. Batooli, A. Vahabzadeh, and J. Trodahl, Appl. Phys. Lett. **100**, 192907 (2012).
[15]G. Singh, V. Sathe, and V. S. Tiwari, J. Appl. Phys. **115**, 044103 (2014).
[16]J. Gao, D. Xue, Y. Wang, D. Wang, L. Zhang, H. Wu, S. Guo, H. Bao, C. Zhou, W. Liu, S. Hou, G. Xiao, and X. Ren, Appl. Phys. Lett. **99**, 092901 (2011).
[17]J. Gao, L. Zhang, D. Xue, T. Kimoto, M. Song, L. Zhong, and X. Ren, J. Appl. Phys. **115**, 054108 (2014).
[18]D. Damjanovic and M. Demartin, J. Phys.: Condens. Matter **9**, 4943 (1997).
[19]D. Damjanovic and M. Demartin, J. Phys. D: Appl. Phys. **29**, 2057 (1996).
[20]N. Bassiri-Gharb, I. Fujii, E. Hong, S. Trolier-McKinstry, D. V. Taylor, and D. Damjanovic, J. Electroceram. **19**, 49 (2007).
[21]J. Fu, R. Z. Zuo, and Z. K. Xu, Appl. Phys. Lett. **99**, 062901 (2011).
[22]R. Theissmann, L. A. Schmitt, J. Kling, R. Schierholz, K. A. Schönau, H. Fuess, M. Knapp, H. Kungl, and M. J. Hoffmann, J. Appl. Phys. **102**, 024111 (2007).
[23]K. A. Schönau, L. A. Schmitt, M. Knapp, H. Fuess, R. A. Eichel, H. Kungl, and M. J. Hoffmann, Phys. Rev. B **75**, 184117 (2007).
[24]H. Wang, J. Zhu, N. Lu, A. A. Bokov, Z. G. Ye, and X. W. Zhang, Appl. Phys. Lett. **89**, 042908 (2006).
[25]F. Bai, J. F. Li, and D. Viehland, Appl. Phys. Lett. **85**(12), 2313 (2004).
[26]W. S. Chang, L. C. Lim, P. Yang, C.-S. Ku, H.-Y. Lee, and C. S. Tu, J. Appl. Phys. **108**, 106102 (2010).
[27]Y. M. Jin, Y. U. Wang, A. G. Khachaturyan, J. F. Li, and D. Viehland, Phys. Rev. Lett. **91**, 197601 (2003).
[28]Y. Sato, T. Hirayama, and Y. Ikuhara, Phys. Rev. Lett. **107**, 187601 (2011).
[29]I. K. Jeong and J. S. Ahn, Appl. Phys. Lett. **101**, 242901 (2012).
[30]J. Ricote, R. W. Whatmore, and D. J. Barber, J. Phys.: Condens. Matter. **12**, 323 (2000).
[31]C. A. Randall, D. J. Barber, and R. W. Whatmore, J. Mater. Sci. **22**, 925 (1987).
[32]M. Tanaka and G. Honjo, J. Phys. Soc. Jpn. **19**, 954 (1964).
[33]B. F. Buxton, J. A. Eades, J. W. Steeds, and G. M. Rackham, Philos. Trans. R. Soc. London A **281**(1301), 171–194 (1976).
[34]Y. Zhang, D. Xue, H. Wu, X. Ding, T. Lookman, and X. Ren, Acta Mater. **71**, 176 (2014).
[35]H. Guo, C. Zhou, X. Ren, and X. Tan, Phys. Rev. B **89**, 100104(R) (2014).
[36]I. Levin, V. Krayzman, and J. C. Woicik, Appl. Phys. Lett. **102**, 162906 (2013).
[37]T. J. Yang, V. Gopalan, P. J. Swart, and U. Mohideen, Phys. Rev. Lett. **82**, 4106 (1999).